

Proceedings of the 40<sup>th</sup> IAHR World Congress 21-25 August 2023 Vienna, Austria DOI number

# Monitoring the Manning's n Coefficient Variation over the Yearly Cycle

M. MUSTE<sup>(1)</sup>, B. CIKMAZ<sup>(1)</sup>, A. LAMOREUX<sup>(1)</sup>, O. BAYDAROGLU YESILKOY<sup>(1)</sup>, I. DEMIR<sup>(1)</sup>, E. MESELHE<sup>(2)</sup>, and C. BACOTIU<sup>(3)</sup>

(1) IIHR-Hydroscience & Engineering, The University of Iowa, Iowa City, Iowa, U.S.A. e-mails: marian-muste@uiowa.edu; atiyebeyza-cikmaz@uiowa.edu; atiyebeyza-cikmaz@uiowa.edu; ozlem-baydaroglu@uiowa.edu; Ibrahim-demir@uiowa.edu

(2) Department of River-Coastal Science and Engineering, Tulane University, New Orleans, U.S.A. e-mail: emeselhe@tulane.edu

(3) Faculty of Building Services Engineering, Technical University of Cluj-Napoca, Cluj-Napoca, Romania e-mail: Ciprian.Bacotiu@insta.utcluj.ro

### **Abstract**

Despite extensive efforts to determine the Manning's n roughness coefficient, its estimation continues to be subjective and clumsy being regarded as the outcome of an intuitive or arbitrary process. Especially complex is the evaluation of vegetation-induced roughness, a time-dependent variable that is difficult to quantify even at one instant. Revisiting the protocols for Manning's coefficient estimation is essential not only to improve a key parameter involved in solving all channel-flow related problems but because the current approaches for its estimation are notoriously unreliable and outdated despite that advances in knowledge and measurement techniques are currently available. This paper describes two evidence-based methodologies for determining the Manning's roughness coefficient using information and data acquired in-situ in a small US Midwestern stream. While these methodologies can be applied to any type of roughness, we focus on vegetation-induced roughness as its evaluation is still considered an open challenge. The methods entail the Continuous Slope-Area method complemented by photo-documentation and synoptic surveys. Monitoring of the "living" roughness associated with the riparian is continuously made over the year to capture its seasonal growth and decay. This monitoring methodology differs from the conventional Manning's n estimation approaches whereby direct measurements are made for specific events and times with estimates provided as average values over ranges of flows and times. The paper describes the settings and measurement protocols associated with the implementation of the hybrid monitoring method and presents preliminary estimations for vegetation-associated roughness during the growing season in spring of 2022.

**Keywords:** Manning's *n* roughness coefficient; vegetation-induced roughness; slope-area method

#### 1. INTRODUCTION

Open-channel flow analyses and computations typically require evaluation of the channel roughness and accounting for it in flow governing equations. From the variety of forms expressing channel roughness, the well-known Manning's n roughness coefficient is often invoked. This coefficient aggregates the effect of channel friction on the flow, hence it is dependent on the flow depth and the boundary texture along the wetted perimeter. Most often the banks of the natural channel banks are covered by vegetation, therefore the bank roughness varies from season to season commensurate with the vegetation age. It should be noted upfront that in channels of small width-to-depth ratios and without vegetation on the bed, the effect of roughness induced by bank vegetation is minimal (Arcement & Schneider, 1989). However, in relatively narrow channels with steep banks, roughness can be significantly affected by the vegetation presence. While the depth change is typically accounted for in roughness estimation, the age of the vegetation is not always considered because of lack of relevant data on its seasonal change.

Conventional practices for estimating channel roughness coefficients include:

- A) indirect estimation from bed descriptions associated with *n*-value tables;
- B) photographs of channels and ancillary descriptions with estimated *n*-value tables;
- C) indirect estimation from various semi-empirical equations; or,

D) direct estimation from known discharges and channel hydraulic properties.

Approaches A and B are generally relying on Approaches C or D for providing actual Manning's *n* values. For example, the roughness values derived from Approach B are tabulated based on a verified *n* value obtained with Approach D computed from known cross-sectional geometry and discharge values at the observation site. Approaches A and B are considered herein qualitative as the selection of the appropriate *n* coefficient is subjective and depends largely on the hydrologist's experience with the subject matter. The Manning's *n* estimation using the Approach D is quantitative being based on measurements with the slope-area (SA) method that was originally introduced by Dalrymple & Benson (1967) for extending the stage-discharge ratings in the area of high flows (ISO:1070, 2018). The values for the Manning coefficient obtained with the above approaches are only valid for the time of collecting the experimental or photo-documentation.

Despite the extensive efforts to comprehensively determine the Manning's roughness coefficient, its estimation continues to be subjective and clumsy being regarded as the outcome of an intuitive or arbitrary process. Especially complex is the evaluation of vegetation-induced roughness, a time-dependent variable that is difficult to quantify even at one instant. From this perspective, revisiting the protocols for Manning's coefficient estimation is essential not only to improve a key parameter involved in solving all channel-flow related problems but because the current approaches for its estimation are notoriously unreliable and outdated despite that advances in knowledge and measurement techniques are currently available.

This study introduces a rigorous, evidence-based methodology for determining the Manning's *n* roughness coefficient by combining Approaches B and D and continuously applying them during the yearly cycle of the vegetation growth and decay. This methodology is easier to access and deploy these days given the availability of low-cost, easily-deployable pressure transducers and the experience with the continuous implementation of the slope-area method for streamflow measurement (e.g., Smith et al, 2010; Stewart et al., 2012). The continuous SA implementation is labeled herein CSA to distinguish from the original SA approach. For this study, we use as a "reference" the estimation Approach B by identifying in published accounts sites that are the closest match to the channel hydro-morphological conditions of our site.

### 2. METHODOLOGY BACKGROUND

**Approach B.** In the preparation phase of this study, a critical review of the publications containing photographic evidence for Manning's *n* coefficient and its rigorous estimation was firstly conducted to identify the most relevant information available for our site characteristics (e.g., Cowan, 1956; Barnes, 1967). From the reviewed sources, we found the study conducted by Coon (1994) as closely matching our research purpose and methodology. This study entailed a large number of sites (31 streams with top-width of 10 to 120 m) displaying a wide range of lengths for the experimental stream reach (from 30 to 400m) and estimation of the roughness coefficient made over several sub-reaches. The contribution of the velocity head in the energy equation used for estimations was neglected based on the assumptions that the difference in velocity heads in carefully selected sites (straight and uniform geometry channels) is negligible. Measurements were made only on flows within the channel banks without significant vegetation growth on the stream bed. Percentage of vegetated areas of the wetted perimeter were taken into consideration for each site and stage. The visual evidence and summary of the Manning's *n* associated with vegetation growth is shown in Figure 1.



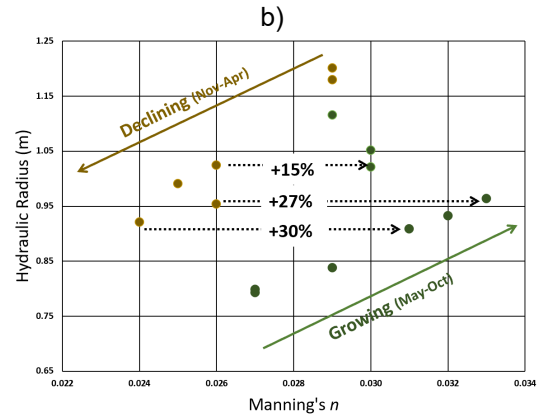


**Figure 1.** Manning *n* variation during the yearly cycle (adapted from Coon, 1994). The banks are covered by grass and vetch with growth of willow saplings at the low-water edge. Bed material: gravel of  $d_{50}$ = 0.02 m.

The information synthesized in Figure 1, illustrate that there is a clear distinction between the roughness coefficient for the same hydraulic radius during periods of vegetation growth and decline. The growing period is associated with the May-October interval while the declining vegetation period is associated with November-April interval. It can be noted that the Manning's n roughness coefficient is systematically larger in

the growing period compared with the declining one. Notable there is a 30% larger roughness in July compared with April (the time stamps are approximative as not all the measurements were dated in the Coon study). Proportional Manning's n increases for the same stage are observable from March to August period (i.e., 27%) and for March – September period (i.e., 15%). The expected roughness increase with the flow depth is observable for all the months displayed in the synthesis plot.

**Approach D.** The estimation method for Manning's *n* coefficient in Coon's (1984) study consists of the slope-area method used in conjunction with known discharge, water-surface profile, and cross sections for the sub-reaches ends. The selection of a suitable site is the most important aspect in the application of the slope-area method as its analytical backbone is the energy equation applied to uniform and steady flow, a situation that occurs in channels that are quasi-prismatic, relatively straight, and maintaining the cross section shape downstream. The preferred governing equation for the implementation of the slope-area method is the Manning equation (Rantz et al., 1982):

$$Q = \left(\frac{1}{n}\right) A R^{\frac{2}{3}} \sqrt{S_f} = K \sqrt{S_f}$$
 [1]

$$S_f = \frac{h_f}{L} = \frac{\Delta h + \Delta h_v - k(\Delta h_v)}{L}$$
 [2]

where n is the Manning's roughness coefficient for the measurement reach of length, L; K is the reach conveyance (estimated as the geometric mean of the conveyance of the two cross-sections bounding the channel reach, i.e.,  $K = \sqrt{K_1 * K_2}$ );  $S_f$  is the friction slope. The friction slope accounts for the difference in water surface elevations at sections 1 and 2, the difference in the velocity head over the reach,  $\Delta h_v$ , and an additional term  $k(\Delta h_v)$  with k being an energy loss coefficient. For lack of better solution, it is assumed that the Manning equation (strictly valid for uniform flow) is also valid for the nonuniform flows. If the channel reach is well selected and short in length, the velocity head difference is small and the friction velocity reduces to  $S_f = (h_1 - h_2)/L$ , where h is the water elevation at the two ends of the channel reach. Under these assumptions the friction slope for non-uniform flow becomes  $S_f = S_0 - \partial h/\partial x$  where  $S_0$  is the channel bed slope. This simplified version of the CSA method was applied by the present authors in several prior studies for both uniform-steady and non-uniform unsteady flows (Lee, et al., 2017; Muste, et al., 2019).

In this paper, we combine the CSA protocol with a suite of contemporary instruments to obtain a continuous relationship between vegetation growth and channel resistance over the yearly cycle complemented by continuous photo-documentation and synoptic vegetation surveys. Documenting such a experimental evidence is important from two perspectives: a) proof-testing a hybrid measurement approach that can be quickly deployed at various representative sites to efficiently track the variation of vegetation-related friction, and, b) better understand the implications of the vegetation impact on channel friction and ultimately on the construction and usage of the rating curves.

### 3. EXPERIMENTAL ARRANGEMENTS

Study site. In this study, we chose the experimental site in the proximity of the USGS gaging station # 05454220 located on the Clear Creek stream near Oxford (lowa, USA) because this site complies with many of the requirements for a good streamflow monitoring site (see Figure 2a). The experimental stream has no lateral inflows or outflows, stays mostly in the main channel, and is not affected by backwater. The channel is geometrically homogeneous (lacking expansions, contractions, and significant bed changes), and it is free of obstructions (logs, debris accumulation) almost continuously. There is no vegetation on the channel bed, but there is abundant vegetation on the banks layered continuously and uniformly over the reach length. The vegetation is also quite well anchored in the banks without significant uprooting or washout episodes. The experimental site was intentionally selected on a small stream with vegetated banks as for such situations the change in the bank roughness due to vegetation growth might become significant. This site has been extensively observed and documented in terms of flow behavior (Lee, 2013; Lee et al., 2017).

Instrumentation setting. The channel free-surface slope was determined every 15 minutes from water elevations recorded by the USGS sensor, a downstream stage sensor (the Bubbler), and two other sensors (i.e., IQ1 and IQ2) that measure stage and index velocity (https://info.xylem.com/sontek-iq-manual.html). Beside the stage, the USGS stage-gaging station also provides discharges via a stage-discharge rating curved developed and maintained by USGS. The Bubbler is an Amazon150-1-00-0 15 PSI pressure sensor (https://www.ysi.com/amazon). All pressures sensors are self-powered and connected to web browsers via Wi-Fi wireless connection. The manufacturer's specification sheet states accuracy ≤ 0.02% of full-scale output over −  $40^{\circ}$  to  $+60^{\circ}$  C temperature range, which in turn is  $\pm$  2.1mm for the 15 PSI sensor measuring up to 10m depth. Prior-to-deployment laboratory measurements in still water confirmed the stated accuracy. The above stated accuracy was sufficient for determining the slope despite that the fall of the free surface between the

sensors was relatively small (up to 0.01m). The pressure sensing probes were installed close to the right bank of the stream (see Figure 2a) and protected by upstream-located poles for deflecting incoming debris. The pressure sensing probes were attached to rigid platforms installed on the riverbed connected to a datalogger with ground-tied flexible tubing.

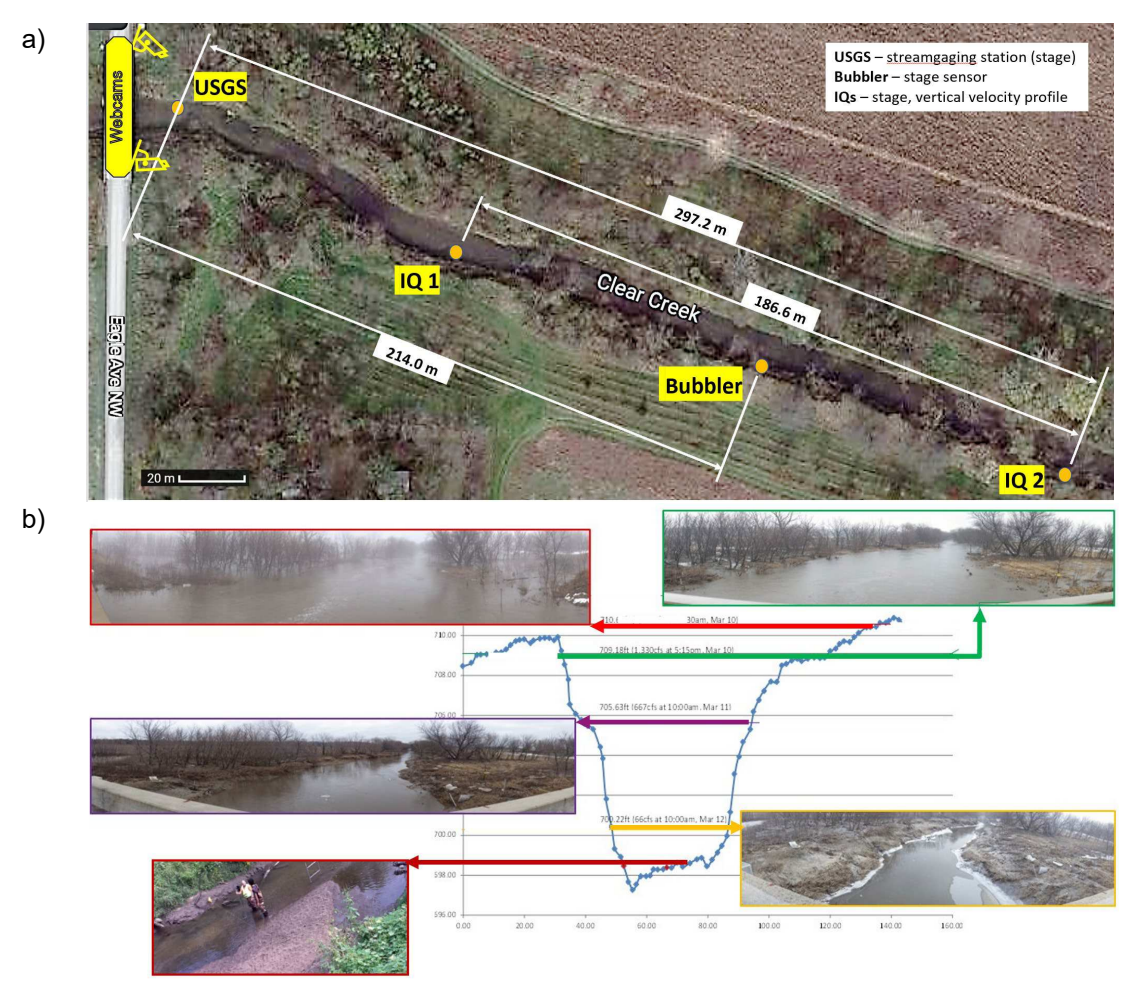


**Figure 2.** Experimental site: a) instrument deployment layout; and, b) photos of actual flows at the site Besides the above-mentioned favorable aspects related to channel geometry, the site was chosen because the stream is relatively small while displaying annually a wide flow range (see Figure 2b).

The photographic documentation of the vegetation growth was accomplished with two webcams mounted on a bridge crossing the stream, as shown in Figure 2a. The framing of both cameras was centered on a set of 14 graduated poles installed in the cross section containing the USGS stage sensor (see Figure 3a). The poles were painted with colored strips 0.152-m tall. The individual location of the poles was surveyed at the time of installation with a total station. While the field of views of the two cameras were overlapping in proportion of 90%, we opted for this arrangement to ensure redundance of the monitoring in case of camera failures and to complement potential obstructions of the pole views during the vegetation growth (see Figure 3b). The webcams have a resolution of 30 MegaPixels, record images as still photos or videos, and are equipped with two-way communication via Modems (https://www.moultriefeeders.com). Daylight photos were taken with the webcam one hour apart throughout the year.

Good practice guidelines recommend the installation of sensors on both sides of channel and a minimum of three cross-sections to address possible changes in the stream geometry. Setting multiple cross sections within the measurement reach can help to determine the slope more accurately (Stewart et al., 2012). The velocity data measured by the two IQs are not processed yet. After the deployment of the stage sensor, a geodetic survey was conducted with a total station to record the water surface elevation above the sensor sensing point. This survey was tied to the geodetic monument located near the USGS gaging station to allow conversion of the water-surface elevations to the North American Vertical Datum of 1988 (NAVD 88). Post-installation surveys (e.g., edge of water along both river sides) and periodic checks of the bubbler system were carried out as described in Muste et al. (2019).

The webcam images provided continuous tracking of the vegetation growth by observing the height of the canopy against the graduated poles. Given that the webcams record distorted images due to the geometrical

perspective, there is a need to convert to real coordinates the height of the vegetation observed in the images at the individual poles. For this purpose, a detailed survey was conducted where the height of the vegetation was carefully assessed through measurements acquired with tapes and with orthogonal close-up photographs. The information collected during the survey was assembled in a calibration plot shown in Figure 3c. The data documenting the vegetation growth with the webcams was bias-corrected for the difference between the actual and webcam surveys. This "calibration' measurements were repeated several times during the monitoring period.

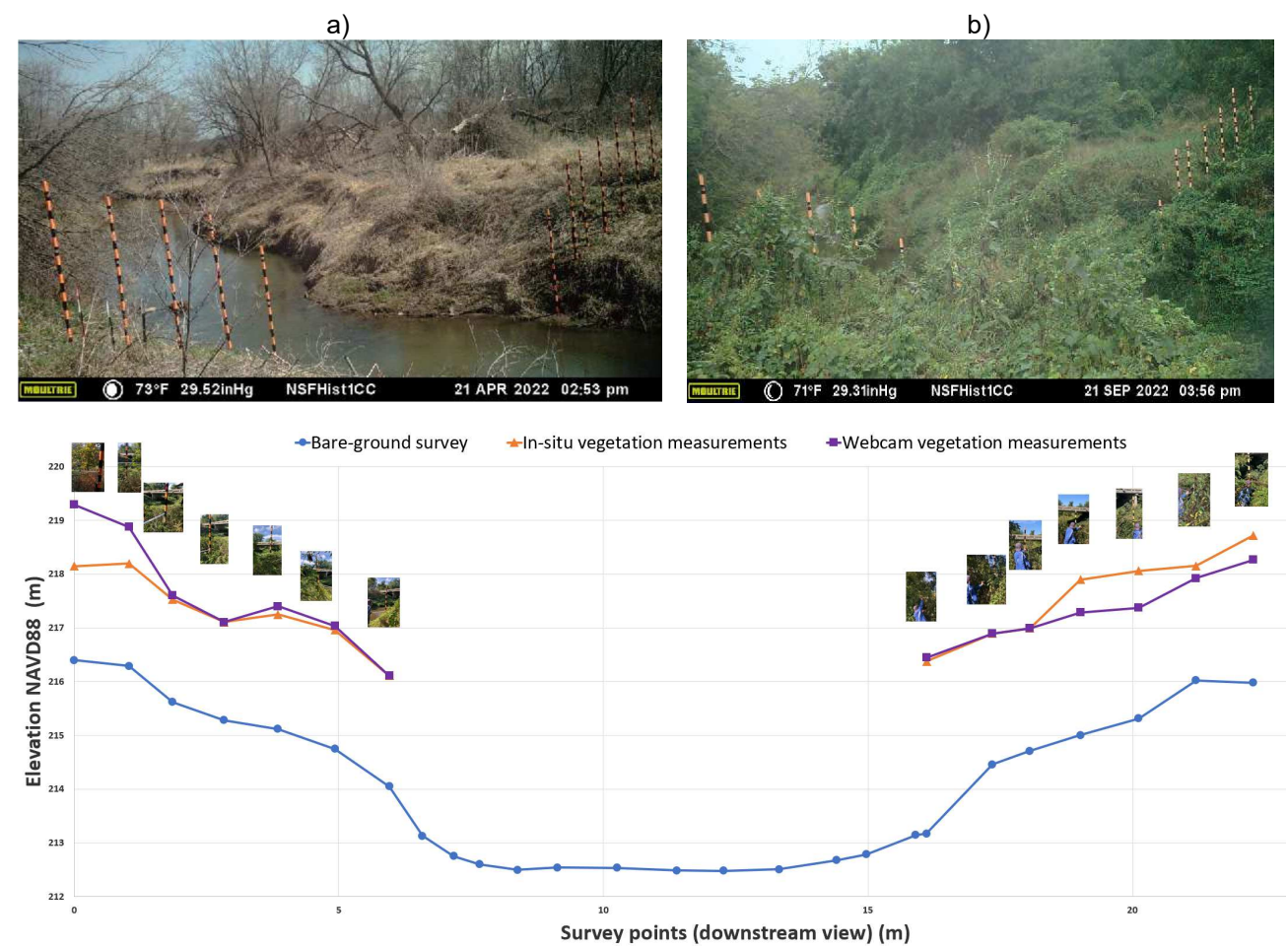


**Figure 3**. Vegetation growth monitored by webcams: a), b) photos captured by webcam #1 on April 21 and September 21, 2022, respectively; and, c) synoptic survey for calibration of the camera images

# 4. DATA ACQUISITION AND PROCESSING PROTOCOLS

The processing protocol presented here is part of broader objective study where we engage simultaneously stage-discharge, index-velocity, and CSA methods. The parallel analysis of these monitoring methods will substantiate the capabilities of the methods to document steady and unsteady flows. Another aspect of this study deals with the protocols for the estimation of the Manning's n roughness coefficient with photographic evidence and look-up table (Approach B) and using the slope- area method (Approach D) collected throughout the yearly cycling of vegetation. While both approaches are used in current practice for Manning's n estimation, the novelty of our protocols is the fact that the monitoring of this "living" roughness is made continuously over the yearly cycle in contrast with conventional methodologies where the estimation is made for specific flow events occurring at specific times and subsequently used as average conditions over a range of flows & times. Presented in this paper are only estimates during the growing season of 2022 from reasons subsequently explained.

**Approach B.** This estimation approach is presented here for the time period April to August, 2022. The view of riparian vegetation growth in this time interval, as documented by the continuous webcamera recordings, is illustrated in Figure 4. While the profiles of the top of the canopy in this figure are self-explanatory, it can be noted that the rates of growth during the April-June time interval are significantly larger than in subsequent months, i.e., July – August when the vegetation reaches maturity. During the site visits for vegetation inspection, sample of the type of vegetation covering the banks were also acquired. This type of

quantitative tracking is not used by the conventional methods for Manning's n estimation. This simple, automated protocol for tracking the riparian vegetation allows one to calculate the composite Manning's n accounting separately for the areas of bed and banks with uniform roughness the (Muste et al. 2019). However, in this discussion, we employ the conventional roughness coefficient estimation approach whereby the photographic evidence of the site of interest at one time instant is associated with tabulated photographs and additional descriptive information for sites where the Manning's n values were estimated through direct measurements applied in the energy equation (i.e., using Approach D). Approach B is extensively used by numerical modelers when calibrating the input for channel roughness in hydrologic models. The results obtained with this traditional approach are presented in the next section.

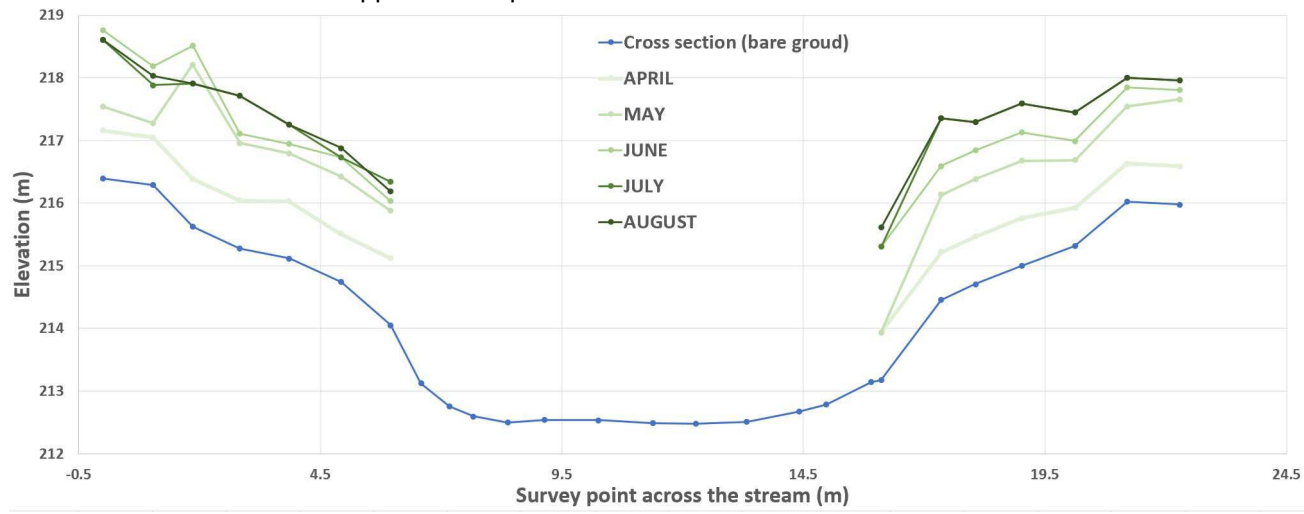


**Figure 4.** Tracking the vegetation status during the growing season at the study site using real-time monitoring system (cross-section corresponding to the USGS stage sensor location)

Approach D. The protocol for implementing Approach D uses the Manning equation with known discharges, stream cross-section geometry for a specific flow, and measured slope of the free surface as surrogate for the friction velocity to back-calculate Manning's n coefficient. At this initial phase of the study, we only can rely for the analysis on the stage-discharge estimates via stage-discharge rating as provided by the USGS #05454220 station as the discharges provided by the slope-area and index-velocity methods are not processed yet. While the stage-discharge ratings are known to be deficient for monitoring unsteady flows, they are still considered close to actual flows on the falling limb of the hydrographs. Of crucial importance for ensuring the reliability of the roughness estimates, is that during the installation and data acquisition the topographic survey of the sensors' tip and the synchronization of all the clocks (instrument and dataloggers) to be carefully set and checked. Small deficiencies in probe survey and synchronization have considerable impacts on the slope magnitude and scattering that can be hardly fixed in post-processing. These cautionary actions are especially important in small stream where the fall of the water surface is small and it can be easily embedded in the instrument noise and naturally occurring fluctuations of the water free surface.

The reference period for documenting the portion of the Manning's *n* associated with the vegetation growth is spanning the time interval from April 24 (deployment date) to July 18, 2022 (see Figure 5). Our analysis is limited to this time span as following July 18, a severe drought left the stream basically flowing close to the zero stage flow until November 11, 2022 (the end of vegetation growth period). During this interval, there were about 5 significant storms recorded at our experimental reach as reflected by the stage time series plotted in Figure 5 at the location of the sensor IQ 1 (shown in Figure 2a). The Spring of 2022 can be considered below the normal ranges of precipitation in the Clear Creek drainage area as indicated by the five storms occurred during the deployment time. Only one event is larger than 214m (corresponding to  $10m^3/s$ ), the threshold stage defining large events at this site (Lee et al., 2017).

Using the above-described instrumentation and data acquisition protocols, the estimation of the progression of the Manning's *n* coefficient in time follows the sequence described below. First, identify points of interest for the analysis so as to capture different vegetation ages. Selection of the set of point of interest is made by crossing the storm hydrographs occurring during the year over a wide range of flow stages at the station, as illustrated in Figure 5. Four points of various stages on the hydrographs associated with storms S1 and S4 are selected from the stage time series recorded during Spring 2022. These analysis points are chosen on the falling limbs of the hydrographs for storm 1 (S1) and storm 4 (S4), as shown in Figure 5. While the protocol described herein can be applied for all five storms plotted in Figure 5, we only present analysis for storms S1 and S4 as they are the largest of the season and quite far apart in time (i.e., April and June).

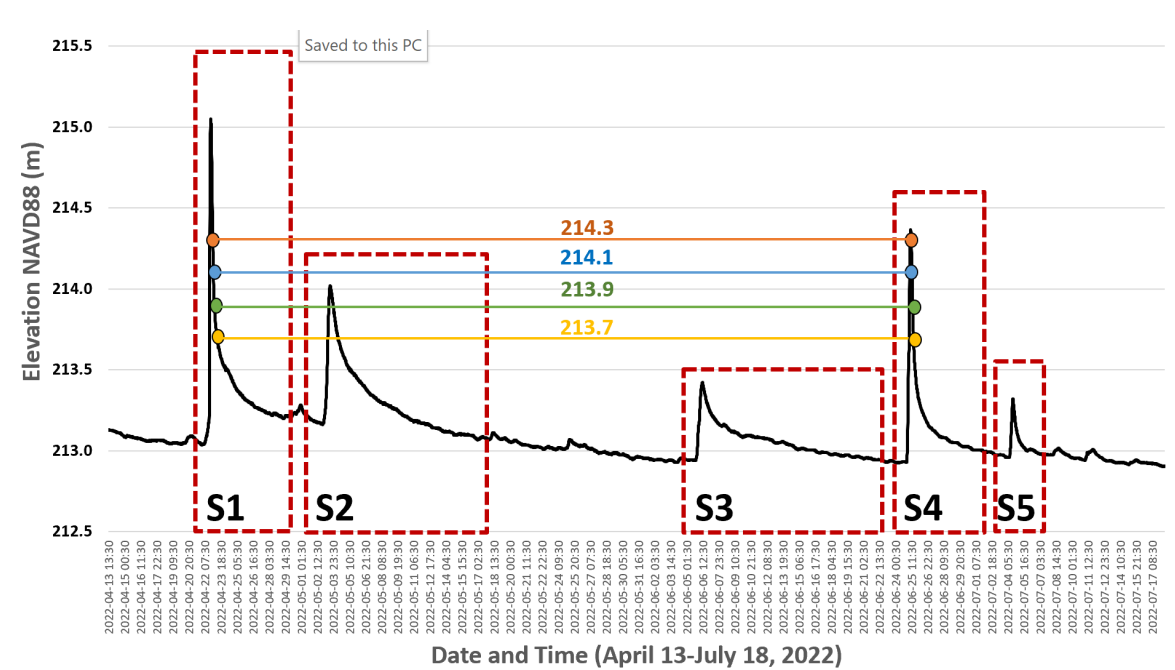


**Figure 5**. Stage dataset recorded at the cross-section IQ 1 during the April 13 -July 18, 2022. Horizontal stage lines identifies the point of analysis (same flow geometry) separated over several months

With the point of interest for the analysis identified, proceed with the following steps:

- record the discharge from the USGS # 054054220 station for the identified points (note that while the
  discharge is constant on the experimental reach, account should be made for the travel time of the
  instantaneous discharge from a stage observation point to the other)
- record water elevations at each end of the CSA experimental reach used for friction slope estimation
- compute cross-section area and the hydraulic radius (from pre-developed ratings as function of stage)
- use the CSA method to back-calculate Manning's *n* coefficient for each identified point of interest.
- catalogue the photograph for each analyzed point and record the relevant metadata (e.g., hydraulic characteristics, descriptions on additional factors that might affect the roughness, special conditions)

Assumption is made that in the reference period, the stream had stable geometry both in the cross sections and over the stream reach length confining the test section. The inspection of all sensor locations and of the experimental reach overall made during the repeated visits at the site are supporting this assumption. In the first phase of the analysis, time instants of identical hydraulic characteristics are identified in the time series and further individually analyzed. We use herein the stage time series for tracking the change in Manning's n over time as this variable is direct measurements not affected by artifacts of additional processing, such is the case with the discharge that is determined from rating curves where additional considerations might be involved.

## 5. PRELIMINARY RESULTS

Approach B. Views of the experimental site in Clear Creek during Spring of 2022 are shown in Figure 6a. Published photographic evidence and tabulated n-values for sites resembling our experimental site are shown in Figures 6b and 6c. These views and relevant information are used to guide the estimation of Manning's *n* at our experimental site. It is obvious from the photographic information and the tabulated information associated with the estimation, that interested users need considerable skills and robust knowledge regarding stream hydraulics to make a decision on the value of the roughness coefficient by accounting for stream characteristics (bed slope, hydraulic specifications, ratio between vegetated and nonvegetated areas on the wetted perimeter, etc.) on one hand, and the photographic evidence on the vegetation characteristics (vegetation type, density and distribution over the bank) on the other hand. The most substantial hurdle in the assessment is that the photographic evidence is not continuous in time. Rather it offers "snapshots" of the site at the time of the quantitative evaluation with the slope-area method. Based on the photographic evidence in the source information with that of our site, we deem that the Manning's *n* value is 0.047 at the end of the growing season. No specifications are provided in the available published source on the flow stage for which the coefficient is estimated. This inferred value is placed at the lower end of the 0.048-0.053 range determined with Approach D for Manning's n estimation during the April – June monitoring interval (see next section).



**Figure 6.** Vegetation growth monitored by webcam #2 at Clear Creek site (USGS stage sensor location), bed slope 0.0004. a) vegetation status before the start of the growing season (March 28, 2022) and during the growing season (June 3, 2022); b) n = 0.047 for Mill Creek (IL), bed slope 0.00047 (September 2004); and, c) n = 0.047 for Rayse Creek (IL), bed slope 0.00044 (September,1999)

Approach D. The view of the measured stages with probes IQ 1 and IQ 2 and of the slopes determined from the data recorded with the pair of stage sensors during the propagation of storms S1 and S4 are illustrated in Figures 7a and 7b, respectively. The maximum fall of the free surface during these events was 0.19 m at the peak of Storm S1, the largest for the reference period. Most of the time, the slope has to be determined from falls less than 0.1m which caused considerable problems for retrieving the actual variation of the stage time series from the noisiness of the recorded signals. Moreover, the two sensors experienced at times bedforms migrating over the probe sensors which created additional noise to the stage measurements and even data drop-outs. Considerable conditioning of the signals and elimination of outliers were needed to make the useful signal visible. Following the data cleaning and conditioning, we obtained the time series for all the variables plotted as 15-minute samples without the need for additional smoothing on the conditioned data points (see Figures 7a and 7b). For verification and validation of the measurements taken in 2022, the time series for the same variables recorded on a storm occurred in 2017 measurement campaign at the same experimental site are replicated in Figure 7c from Muste et al. (2019). The inclusion of this figure is considered relevant because, coincidentally, the storm event has the same magnitude but slightly higher storm intensity (ratio of storm magnitude to propagation duration) and almost all the measurement elements were quite similar in 2017 compared with the 2022 deployment.

The most important result of the present analysis is illustrated in Figure 7d where the estimates of the Manning's n coefficient using Approach D for the four homologous points (i.e., recorded at the same stage value) during storms S1 and S4 are shown. The values of the roughness coefficient estimated with direct measurements display all the essential features looked for in the study: a) clear dependence of the roughness coefficient with the stage increase; and, b) a slight increase (i.e., less than 8%) in the roughness coefficient from late April to late June. The magnitude of the change in roughness coefficient is not more substantial given that the stages for the four homologous points during Storms S1 and S4 are barely protruding into the vegetated banks (see Figure 4). An unexpected feature revealed by this plot is that the percentage increase in roughness is larger in the lower stage area. Previous estimations of Manning's n roughness coefficients at this site during the growing season were ranging from 0.03-0.055 for stages between 213 to 216.5 m.

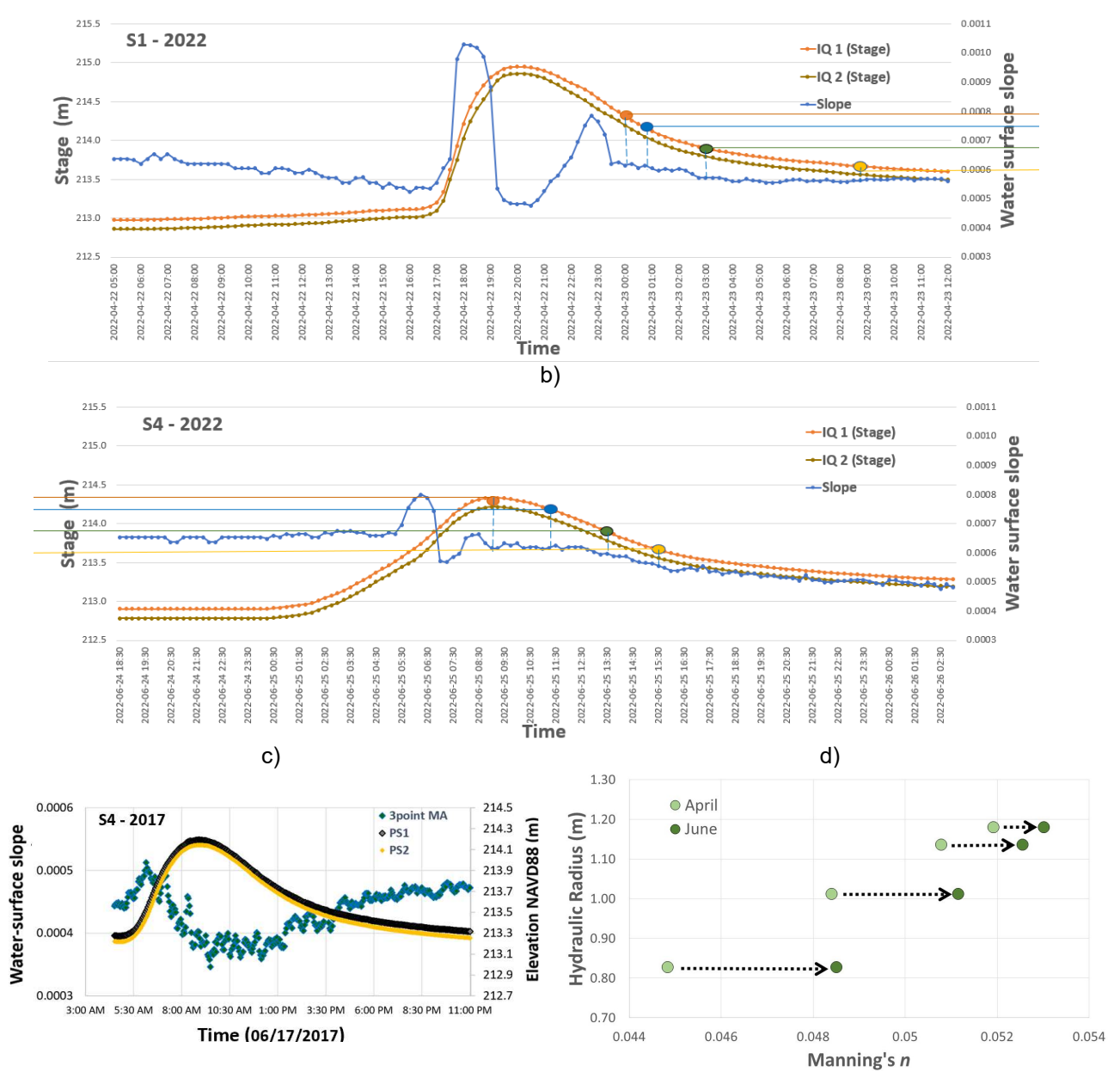


Figure 7. Results obtained with Approach D: a) time series of the stages and slopes determined from the IQ 1 and IQ 2 stage sensors during storms S1 and S4, 2022; c) same dependencies as in Figures 7a and 7b acquired with different instruments and probe locations during a storm propagating through the same experimental reach in 2017; d) estimates of the Manning's *n* coefficient for the April-June, 2022 interval

The obtained results show some level of scattering, but they are within satisfactory ranges. This conclusion is drawn based on information garnered from previous experience with the slope-area method. Published accounts indicate that the slope-area method accuracy is limited to perhaps 15% for typical applications to lowland rivers (Barnes, 1967; ISO 1070, 2018). From this perspective, the results reported herein should be considered indicative rather than definitive. Final estimates for representative roughness coefficient accounting for vegetation growth require repetition of the direct measurement campaigns over a series of storm events occurring over a range of vegetation age with continuously optimized instrumentation and deployment protocols.

# 6. CONCLUSIONS

The paper presents a method for real-time estimation of the Manning's roughness coefficient, n, a critical open-channel flow parameter that is essential both in discharge monitoring (via rating curves that are relying on Manning equation to guide the rating construction) as well as for modeling of open-channel flows. While not new from the point of view of underlying principles, the protocols used for method implementation are

novel in that it tracks quantitatively and qualitatively the multiple factors associated with the change in the roughness coefficient during the vegetation seasonal cycling. It does so by taking advantage of the new generation of digital instruments and communication means. The initial phases of the processing of the acquired data brought in attention a series of issues to be considered into the future for pursuing such in-situ estimations. The most important among these issues are: a) increasing the data sampling frequencies, b) perfecting procedures for time synchronization between the probe sampling and datalogger recording, c) improving the accuracy of the probe surveys, and, d) determining optimal distance between the sensors used for the slope measurement. Regarding the latter issue, a trade off based on analytical predictions is needed to correlate the type of events occurring at the site (available from prior monitoring), the celerity of flood wave propagation, and the sensitivity of the instruments measuring the stage over various distances.

We envision that this method can be applied at relevant observation points in the stream network using, what we deem to be a simple to deploy, relatively cost-efficient measurement installation. The method can be designed as a portable system with deployment durations commensurate with large flood wave events propagating in different seasons. The deployment programs should be based on a matrix for stream characterization based on regional factors (soil, climate, vegetation characteristics) associated with the temporary deployments at various representative locations. Given the complexity of the measurements and the weather variability, it is emphasized that organization of multi-year monitoring campaigns is also of essence for the generalization of the estimates to other locations.

#### 7. ACKNOWLEDGEMENTS

The first six co-authors acknowledge the financial support provided for this research by the NSF EAR-HS 2139649 award.

#### 8. REFERENCES

- Arcement, G.J., Jr. and Schneider, V.R. (1989). Guide for selecting Manning's roughness coefficients for natural channels and flood plains, *U.S. Geological Survey Water-Supply Paper* 2339, 38 p.
- Barnes, H.H. (1967). Roughness characteristics of natural channels, *U.S. Geological Survey Water-Supply Paper* 1849, 213 p.
- Bathurst, J.C. (1986). Slope-area discharge gaging in mountain rivers, *Journal of Hydraulic Engineering*, 112 (5) ISSN 0733-9429/86/0005-0376/\$01.00. Paper No. 20619, pp. 376-391.
- Coon, W. F. (1994). Estimation of roughness coefficients for natural stream channels with vegetated banks, *U.S. Geological Survey water-supply paper* 2441, DOI: doi.org/10.3133/wsp2441
- Cowan, W.L. (1956). Estimating hydraulic roughness coefficients, Agricultural Engineering, 37(7), 473-475.
- Dalrymple T., Benson M.A., (1984). Measurement of peak discharge by the slope—area method, *U. S. Geological Survey Techniques of Water-Resources Investigations*, Book 3, Chapter A2, p. 12
- ISO 1070 (2018). Liquid Flow Measurement in Open Channels—Slope-Area Method," Measurement of Liquid Flow in Open Channels, *ISO Standards Handbook*, International Organization for Standardization, Geneva, Switzerland.
- Lee, K. (2013). Evaluation of methodologies for continuous discharge monitoring in unsteady open-channel flows, *PhD Dissertation*, The University of Iowa, Iowa City, Iowa, U.S.A.
- Lee, K., Firoozfar, A. R., & Muste, M. (2017). Monitoring of unsteady open channel flows using the continuous slope-area method, *Hydrology & Earth System Sciences*, 21(3).
- Muste, M., Bacotiu, C., & Thomas, D. (2019). Evaluation of the slope-area method for continuous streamflow monitoring. *Proceedings of the 38th IAHR World Congress*, Panama City, Panama
- Rantz, S. E. (1982). Measurement and computation of streamflow (Vol. 2175): *US Department of the Interior, Geological Survey*, Vol. I.
- Smith, C.F., Cordova, J.T., and Wiele, S.M. (2010). The continuous slope-area method for computing event hydrographs: *U.S. Geological Survey Scientific Investigations Report* 2010-5241, 37 p.
- Soong, D.R., Prater, C.D., Halfar, T.M. and Wobig, L.A. (2012) Estimating Manning's Roughness Coefficients for Natural and Man-Made Streams in Illinois, *Joint study by U.S. Geological Survey-Illinois Water Science Center and the Illinois Department of Natural Resources-Office of Water Resources* (available online at: https://il.water.usgs.gov/proj/nvalues)
- Stewart, A. M., Callegary, J. B., Smith, C. F., Gupta, H. V., Leenhouts, J. M., & Fritzinger, R. A. (2012). Use of the continuous slope-area method to estimate runoff in a network of ephemeral channels, southeast Arizona, USA. *Journal of Hydrology*, 472, 148-158.